UNIVERSIDADE DE SÃO PAULO

INSTITUTO DE FÍSICA
CAIXA POSTAL 20516
01498 SÃO PAULO - SP
BRASIL

PUBLICAÇÕES

IFUSP/P-970

SIMPLE APPROXIMATION TO CONTINUUM RANDOM PHASE APPROXIMATION (RPA): APPLICATION TO THE GIANT DIPOLE RESONANCE IN ^{16}O

N. Teruya
Departamento de Física, Universidade Federal da Paraíba
C.P. 5008, 58059 João Pessoa, PB, Brasil

H. Dias and **A.F.R. de Toledo Piza**
Instituto de Física, Universidade de São Paulo

Fevereiro/1992

SIMPLE APPROXIMATION TO CONTINUUM RANDOM PHASE APPROXIMATION (RPA): APPLICATION TO THE GIANT DIPOLE RESONANCE IN ^{16}O

N. Teruya

Departamento de Física, Universidade Federal da Paraíba
C.P. 5008, 58059 João Pessoa, PB, Brasil

H. Dias and **A.F.R. de Toledo Piza**

Instituto de Física, Universidade de São Paulo
C.P. 20516, 01498 São Paulo, SP, Brasil

ABSTRACT

We implement a reaction-theory based version of the continuum Random Phase Approximation (RPA) approach to the microscopic structure of nuclear giant resonances in its simplest form. This involves a discrete RPA diagonalization of standard size but involving complex matrices so as to account for single-particle resonance widths. Escape widths of individual resonant structures in the case of the giant $E1$ strength in ^{16}O are obtained in reasonable agreement with available data. The overall strength distribution agrees with that obtained in brute-force continuum RPA calculations.

I. INTRODUCTION

The features of nuclear giant resonances have been studied for a long time in order to understand the structure and dynamics of these excitation modes and, in particular, the relative importance of two different spreading mechanisms for the collective strength, namely continuum spreading, due to direct coupling to the available open channels, and many-body spreading, due to coupling to other nearby noncollective modes. Actually these two mechanisms put quite distinct demand pressures on available microscopic computational techniques, such as those based on the Random Phase Approximation (RPA). While interest in the many-body mechanism led to the consideration of "higher" forms of the RPA, i.e., involving two-particle, two-hole excitation operators in addition to the standard particle-hole excitations, work concerning the consideration of continuum spreading concentrated in developing computational tools to deal efficiently with the particle-hole continuum.

The inclusion of continuum effects in microscopic nuclear structure calculations has in fact been implemented several times, in the context of different frameworks. Besides continuum extensions of the RPA[1–4], use has been made of coupled channels[5] and time-dependent Hartree-Fock calculations[6]. Although successful in the sense of producing sensible strength distributions, these calculations are however not able to identify in microscopic terms the nature of the more or less autonomous resonant structures together with their corresponding relevant parameters, notably individual escape widths. To some extent, more recent calculations aimed at eliminating these drawbacks, equipping themselves with the ability to identify specific resonant features[7–10]. Here we explore one particular approach of this type[11], which is closely linked to a comprehensive nuclear reaction theory. Because of this, the way is in principle open for the consideration of dynamical complications such as preequilibrium processes and compound nucleus formation (related to many-body spreading) or direct channel coupling effects[12]. We concentrate, however, in demonstrating by means of a simple application to the giant $E1$ strength in ^{16}O, the capability of the method to produce detailed microscopic information on the continuum resonant structures at a very modest computational cost. This last circumstance provides for the necessary encouragement to extend the method to accommodate more comprehensive dynamics.

For the sake of completeness, the scheme proposed in ref. [11] is briefly reviewed in section II below. Section III describes the results of our calculations, and concluding remarks are presented in section IV.

II. REVIEW OF CALCULATION SCHEME

Before presenting numerical results we briefly review the scheme proposed in ref. [11] for the calculation of the continuum particle-hole response. The aim is to obtain an approximation to the (retarded) response function ($\hbar = 1$) [13]

$$(12|R(\omega)|1'2') = \sum_c \sum\!\!\!\!\!\!\int_{E_\nu>0} \left[\frac{\langle 0|\psi_2^\dagger \psi_1|\nu^{(c)\dagger}\rangle\langle \nu^{(c)\dagger}|\psi_{1'}^\dagger \psi_{2'}|0\rangle}{\omega - E_\nu + i\eta} - \right.$$

$$\left. - \frac{\langle 0|\psi_{1'}^\dagger \psi_{2'}|\nu^{(c)\dagger}\rangle\langle \nu^{(c)\dagger}|\psi_2^\dagger \psi_1|0\rangle}{\omega + E_\nu + i\eta}\right] \qquad (2.1)$$

where the ψ_i, $\psi_i^\dagger$ are fermion field operators. The matrix elements involve the ground state (with energy eigenvalue set to zero by definition) and excited states $|\nu\rangle$ with energy eigenvalues E_ν. When lying in the continuum they are subject to scattering boundary conditions involving incoming flux in channel c and outgoing waves in all channels. As in the ordinary RPA scheme, approximate excited states will be implemented in the particle-hole excitation space of $|0\rangle$. Open channels will thus correspond to unbound particle-hole states. We assume a model Hamiltonian

of the form

$$H = H_0 + \frac{1}{2}\sum_{ij} V_{ij}$$

involving a mean-field part H_0 and a (residual) two-body force.

A main point concerns the handling of the single-particle continuum

$$[\epsilon - H_0]\,|\alpha_\epsilon^{(\dagger)}\rangle = 0 \ .$$

To this effect we split the single-particle phase space by means of a pair of complementary projection operators $q = q^\dagger = q^2$ and $p = p^\dagger = p^2$ so that

$$|\alpha_\epsilon^\dagger\rangle = q|\alpha_\epsilon^\dagger\rangle + p|\alpha_\epsilon^\dagger\rangle \ .$$

The component $q|\alpha_\epsilon^\dagger\rangle$ has finite norm and is chosen so as to contain the resonant behavior of the continuum wavefunction in the nuclear interior. The remaining component is correspondingly small there, having negligible (to a first approximation) matrix elements with hole (bound) wavefunctions. The numerical implementation of this projection scheme has been described in detail in ref. [14], which essentially elaborates on the technique discussed long ago by Wang and Shakin[14]. The coupling between q and p subspaces gives rise to the single-particle resonance width. It is accounted for, within the discrete q subspace, through the familiar complex effective Hamiltonian

$$\hat{H}_{0qq} = H_{0qq} + H_{0qp}\left(\epsilon^\dagger - H_{0pp}\right)^{-1} H_{0pq} \ .$$

As shown in ref. [13], one can use this Hamiltonian to obtain a discrete set of normalized resonance wavefunctions with complex energies, of which the imaginary parts account for the single-particle escape widths.

Our continuum approximation then proceeds as follows. Using the above analysis of the single-particle space one can split also the particle hole space with help of a pair of complementary projectors $Q = Q^\dagger = Q^2$ and $P = P^\dagger = P^2$ onto normalized resonance (q-space)-hole and residual continuum (p-space)-hole states respectively. Possible bound-particle-hole states are also included in Q. The relevant approximate excited states for eq. (2.1)are then to be found as solutions of the coupled equations

$$[E_\nu - H_{QQ}]\, Q|\nu\rangle = H_{QP}\, P|\nu\rangle$$

$$[E_\nu - H_{PP}]\, P|\nu\rangle = H_{PQ}\, Q|\nu\rangle$$

supplemented with the appropriate boundary conditions. When the incoming flux is in channel c we have

$$\left[E_\nu - H_{QQ} - H_{QP}\,\frac{1}{E_\nu + i\eta - H_{PP}}\,H_{PQ}\right] Q|\nu\rangle = H_{QP}|\chi_c^\dagger\rangle \qquad (2.2)$$

where $|\chi_c^\dagger\rangle$ is the appropriate scattering solution of H_{PP}:

$$[E_\nu - H_{PP}]\,|\chi_c^\dagger\rangle \quad . \qquad (2.3)$$

In order to handle these equations we invoke the quenching of p-space wavefunctions in the nuclear interior to ignore effects of the two-body force in H_{QP} (and H_{PQ}) and in H_{PP}. Eq. (2.3) is thus a single-particle equation (the hole is passive), and the continuum selfenergy

$$H_{0QP}\,\frac{1}{E_\nu + i\eta - H_{0PP}}\,H_{0PQ}$$

dresses single-particle resonance energies with escape effects (shifts and widths). Similarly, we neglect the contribution to the matrix elements entering in eq. (2.1) of the components $P|\nu\rangle$. Eq. (2.1) can therefore be evaluated in terms of the solutions to eq. (2.2), which can be written as

$$Q|\nu\rangle = \sum_n \frac{|R_n\rangle\langle\tilde{R}_n|H_{PQ}|\chi_c^\dagger\rangle}{E_\nu - \hat{\epsilon}_n} \qquad (2.4)$$

$$\left[\hat{\epsilon}_n - \hat{H}_{QQ}\right]|R_n\rangle = 0 \qquad (2.5a)$$

$$\left[\hat{\epsilon}_n^* - \hat{H}_{QQ}^\dagger\right]|\tilde{R}_n\rangle = 0 \qquad (2.5b)$$

$$\langle\tilde{R}_{n'}|R_n\rangle = \delta_{nn'} \quad .$$

Eqs. (2.5) involve the complex effective Hamiltonian appearing in eq. (2.2) and its adjoin. The complex particle-hole modes $|R_n\rangle$ have complex energies $\hat{\epsilon}_n$ which account for continuum escape effects. They can be described therefore in terms of an approximate continuum Tamm-Dancoff scheme.

In the numerical results reported below this scheme is in fact replaced by an RPA diagonalization in Q-space. Thus, instead of eqs. (2.5) we solve

$$\hat{\epsilon}_n \mathbb{G}\mathbb{R}^{(n)} = \varepsilon\,\mathbb{G}\mathbb{R}^{(n)} + \mathbb{G}\mathbb{M}\,\mathbb{G}\mathbb{R}^{(n)} \qquad (2.6a)$$

$$\hat{\epsilon}_n^*\,\mathbb{G}\tilde{\mathbb{R}}^{(n)} = \varepsilon^\dagger\,\mathbb{G}\tilde{\mathbb{R}}^{(n)} + \mathbb{G}\mathbb{M}\,\mathbb{G}\tilde{\mathbb{R}}^{(n)} \qquad (2.6b)$$

where $\mathbb{G}_{\alpha\beta;\gamma\delta} = (p_\beta - p_\alpha)\,\delta_{\alpha\gamma}\,\delta_{\delta\beta}$, the p_α being the occupation numbers (0 or 1) of the single-particle states α in $|0\rangle$, and

$$\varepsilon_{\alpha\beta;\gamma\delta} = (\hat{\epsilon}_\alpha - \hat{\epsilon}_\beta)\,\delta_{\alpha\gamma}\,\delta_{\beta\delta} \quad ,$$

the $\hat{\epsilon}_\alpha$ being single-particle energies. They are complex for resonance states. The coupling matrix $\mathbb{M}$ is given as

$$\mathbb{M}_{\alpha\beta;\gamma\delta} = \langle\alpha\delta|\nu|\beta\gamma - \gamma\beta\rangle \quad .$$

Note that the matrix element involving $\langle\tilde{R}_n|$ in eq. (2.4) is in fact an escape amplitude, related to the imaginary part of $\hat{\epsilon}_n$. The mode $|R_n\rangle$ in $Q|\nu\rangle$ is therefore weighted by an amplitude of Breit-Wigner form which accounts for the continuum spreading of the mode. When this spreading is negligible, the contribution of $|R_n\rangle$ to the response tends to reduce to a δ-function at the corresponding excitation energy.

We also evaluate the energy weighted strength for the multipole operator Q_λ as

$$S(Q_\lambda\,;\,E) \;=\; \int_0^E dE_\nu\, E_\nu\, |\langle\, \nu|Q_\lambda|0\,\rangle|^2 \qquad (2.7)$$

where $|\nu\rangle$ is replaced by eq. (2.4). As a consequence of the preceding remarks this function approximates a series of steps at the excitation energies $\hat{\epsilon}_n$ in the case of negligible continuum spreading. An effect of the continuum spreading is the smoothing of this discontinuous behavior.

A question of principle deserving special comment is that the effective hamiltonians resulting from the projection approach are explicitly energy dependent (see e.g. eq. (2.2)). This has been repeatedly handled in practice by invoking the smooth energy dependence of the projected continuum propagator $(E + i\eta - H_{0PP})^{-1}$, and this is certainly applicable in the context of the Tamm-Dancoff framework set by eqs. (2.5). A somewhat more serious situation develops, however, when one moves from eqs. (2.5) to the corresponding RPA diagonalization, eqs. (2.6). The purpose of this modification of the secular problem is, as is well known, to allow for at least a restricted class of quantum vacuum fluctuations also known as RPA ground state correlations. This is achieved through a doubling of the quantum phase-space allowing also for negative energy solutions of the dynamical equations, certainly a hazardous situation when one is already dealing with an energy-dependent effective hamiltonian. Actually, an alternate approach to the projected RPA scheme is possible. It consists in implementing the P-Q analysis of the quantum phase space on the full continuum diagonalization problem *after* it has been cast in RPA form. This is analogous to the use of projection techniques to reduce the response function obtained in the framework of "higher" versions of the RPA[15], and leads to an effective RPA matrix in which the backward going particle-hole processes

involve single particle energies dressed with self-energies involving $(E + H_{0PP})^{-1}$, consequently suppressing the respective imaginary parts, in particular.

This difficulty of principle stems ultimately from a basic incongruence between the projection method and the standard RPA space doubling trick. It may be noted, however, that it is of little *practical* consequence at least in the context of hard collective modes such as the giant multipole resonances. Here, in fact, RPA ground state correlation (backward) effects are at least one order of magnitude down with respect to the forward effects. Self-energy uncertainties in the backward processes, notably imaginary parts related to escape effects are in turn typically smaller than the involved single-particle energies, and thus unable to affect collective escape widths significantly.

III. NUMERICAL RESULTS: GIANT $E1$ MODES IN ^{16}O

We have performed the RPA calculations with a Landau-Migdal particle-hole force similar to that of ref. 3. The overall strength parameter C_0 is set so as to give the spurious isoscalar dipole mode essentially at zero energy and the lowest 3^- state approximately at the 6.13 MeV experimental energy[16]. We obtained the constant $C_0 = 415$ MeV fm^3 with the lowest 3^- state at 6.16 MeV. This adjustment provides a constant C_0 only slightly different from that used in the full continuum calculation of ref. [14] ($C_0 = 418.852$ MeV fm^3). We utilized a p-h basis including single-particle states up to the $3s_{1/2}$ (resonance) level calculated as in ref. [13]. Our results are presented in figs. 1 and 2 where we display the functions $dS/dE\ (Q_\lambda\,,E)$ and $S(Q_\lambda\,,E)$, respectively. The most prominent contributions to the $E1$ strength are shown in Table 1 where the imaginary part of the energies are interpreted as the half values of the escape widths ($\Gamma^{\uparrow}$). These results are in good agreement with the calculations of ref. [3] that have the two main peaks at 24.9 and 26.2 MeV but if we compare with the experimental[17] results (22.15 MeV and $\Gamma^{\uparrow} = 1.6$ MeV) our results are shifted upwards in energy by ~ 2.0 MeV. The escape width $\Gamma^{\uparrow}$ is in good agreement with the observed experimental width. Fig. 2 shows that the function $S(Q_\lambda, E)$ exhaust approximately 91% of the classical sum rule[18] for $E = 30$ MeV which is in fairly good agreement with the calculations in ref. [3]. Our results are also in good agreement with the RPA calculations in ref. [1] where the Skyrme interaction SIII is used.

A final remark concerns the calculation of ref. [8], which, like our calculation, involves the consideration of a discrete set of resonance states. Here, however, the definition of these states is based on a formal procedure which beclouds their connection with the underlying many-body scattering problem. As a result of this complex values are produced for the energy-weighted strength. This rather unwelcome feature is an artifact of that procedure which is naturally avoided in the present approach.

IV. CONCLUDING REMARKS

The results of the calculation described in section III show that the approximation scheme proposed in ref. [11] and reviewed in section II above is able to produce results compatible with full continuum calculations as performed e.g. in ref. [3] but at a substantially lower level of computational effort and keeping the underlying physics under ready control. In particular, the adopted formulation easily allows for the inclusion of more complicated dynamical effects, such as e.g. direct couplings between open channels, at the expense of setting up descriptions of scattering states more sophisticated than the extreme single-particle limit adopted here[11].

REFERENCES

[1] F. Liu and N. Van Giai, *Phys. Lett.* **65B**, 23 (1976).

[2] S. Shlomo and G. Bertsch, *Nucl. Phys.* **A243**, 507 (1975).

[3] R. de Haro, S. Krewald and J. Speth, *Nucl. Phys.* **A388**, 265 (1982).

[4] Ph. Chomaz, N. Van Giai and S. Stringari, *Phys. Lett.* **189B**, 375 (1987).

[5] B. Buck and A.D. Hill, *Nucl. Phys.* **A95**, 271 (1967).

[6] S. Stringari and D. Vautherin, *Phys. Lett.* **88B**, 1 (1979).

[7] N. Van Giai, P.F. Bortignon, F. Zardi and R.A. Broglia, *Phys. Lett.* **B199**, 155 (1987).

[8] P. Curutchet, T. Vertse and R.J. Liotta, *Phys. Rev.* **C39**, 1020 (1989).

[9] F. Zardi and P.F. Bortignon, *Europhys. Lett.* **1**, 281 (1986).

[10] S. Yoshida and S. Adachi, *Z. Phys.* **A325**, 441 (1986).

[11] A.F.R. de Toledo Piza, *Rev. Bras. Fis.* **17**, 195 (1987).

[12] G.A. Foglia and A.F.R. de Toledo Piza, Proc. of the 1989 Nuclear Physics Conference, Vol. 2, World Scientific (1990), p. 453.

[13] P. Ring and P. Schuck, *The Nuclear Many-Body Problem.*, Springer 1980, p. 318.

[14] N. Teruya, A.F.R. de Toledo Piza and H. Dias, *Phys. Rev.* **C44**, 537 (1991); W.L. Wang and C.M. Shakin, *Phys. Lett.* **32B**, 421 (1970).

[15] K. Takayanagi, K. Shimizu and A. Arime, *Nucl. Phys.* **A477**, 205 (1988).

[16] F. Ajzemberg-Selove, *Nucl. Phys.* **A460**, 1 (1986).

[17] J.R. Calarco, S.W. Wissink, M. Sasao, K. Wienhard and S.S. Hanna, *Phys. Rev. Lett.* **39**, 925 (1977).

[18] H. Vi and T. Tsukamoto, *Prog. Theor. Phys.* **51**, 1377 (1974).

TABLE CAPTION

Table 1. Energies and widths of the three most prominent $E1$ complex modes calculated using eqs. (2.6) with a Landau-Migdal residual interaction with $C_0 = 415$ MeV fm^3. See fig. 1 for the respective $E1$ strengths.

FIGURE CAPTIONS

Figure 1. Energy differential strength $dS(E1;E)/dE$ (see eq. (2.7)). Normalization is such that $S(E1;\infty) = 1$.

Figure 2. Integrated relative $E1$ strength $\left(\frac{E\cdot|S(E)|^2}{\int_0^\infty E\cdot|S(E)|^2\,dE} \times 100\right)$ in ^{16}O.

Table 1

ε_n =	ε_n	−	$\frac{i}{2}\Gamma_n^{\uparrow}$	in MeV
	17.01	−	i 0.45	
	24.17	−	i 0.72	
	25.40	−	i 0.42	

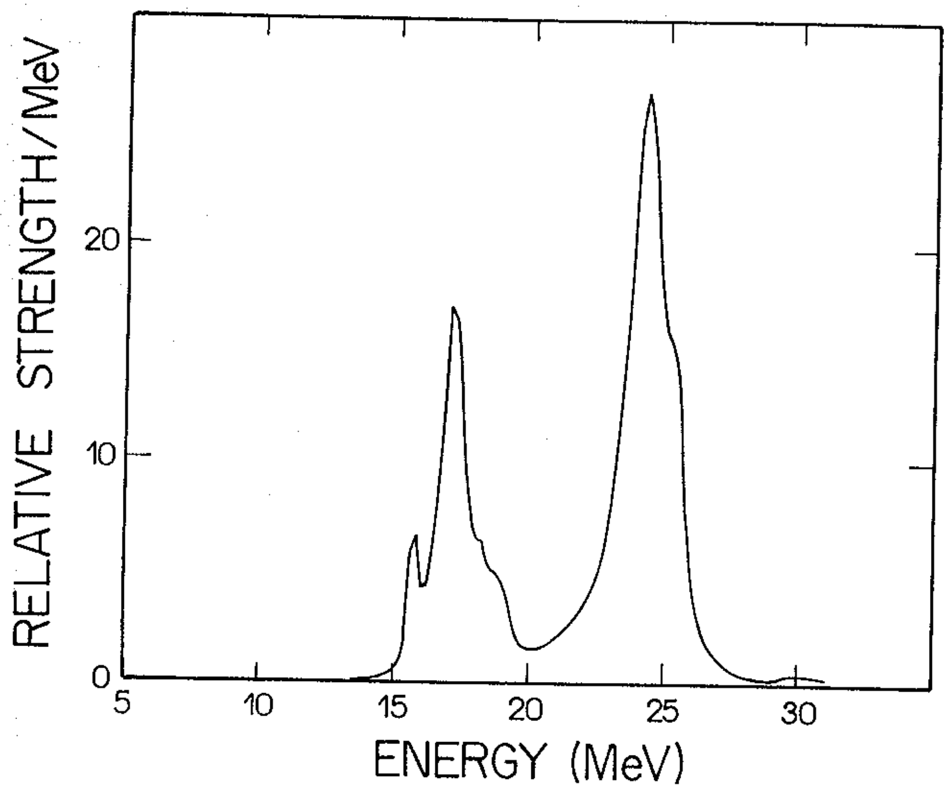

FIGURE 1

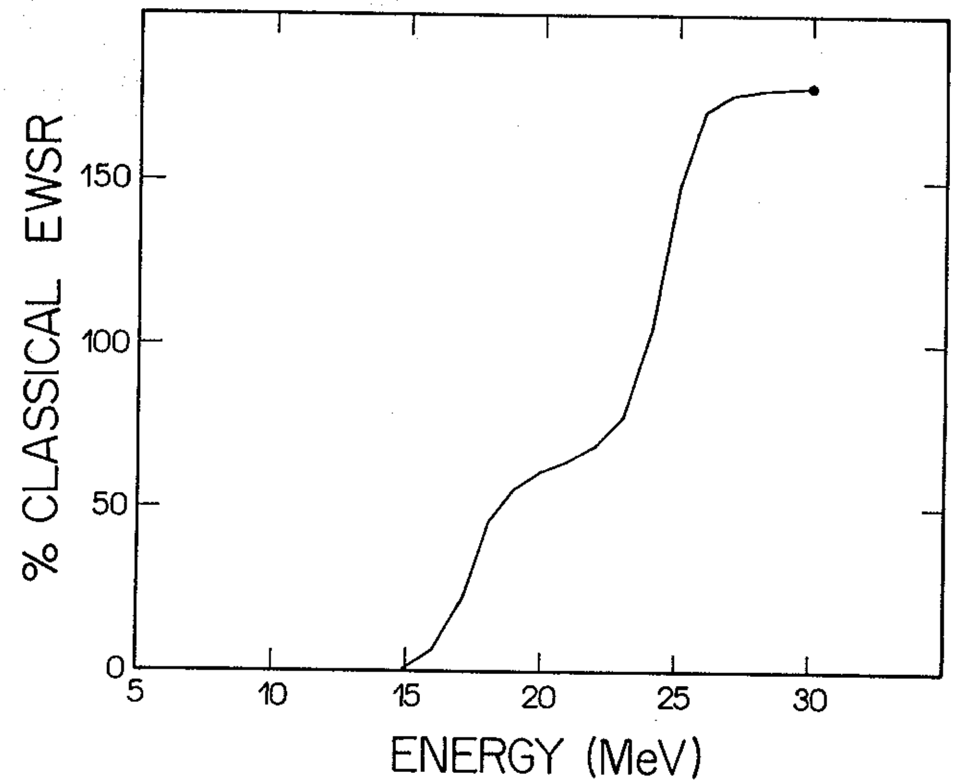

FIGURE 2